

# Do grain boundaries matter? Electrical and elemental identification at grain boundaries in LeTID-affected *p*-type multicrystalline silicon

Mallory A. Jensen<sup>1</sup>, Ashley E. Morishige<sup>1</sup>, Sagnik Chakraborty<sup>2</sup>, Romika Sharma<sup>2</sup>, Hang Cheong Sio<sup>3</sup>, Chang Sun<sup>3</sup>, Barry Lai<sup>4</sup>, Volker Rose<sup>4,5</sup>, Amanda Youssef<sup>1</sup>, Erin E. Looney<sup>1</sup>, Sarah Wieghold<sup>1</sup>, Jeremy Poindexter<sup>1</sup>, Juan-Pablo Correa-Baena<sup>1</sup>, Daniel Macdonald<sup>3</sup>, Joel B. Li<sup>2</sup>, Tonio Buonassisi<sup>1</sup>

<sup>1</sup>Massachusetts Institute of Technology, Cambridge, MA 02139, USA, email: jensenma@alum.mit.edu

<sup>2</sup>Solar Energy Research Institute of Singapore, Singapore 117574, Singapore

<sup>3</sup>Australian National University, Canberra, ACT 0200, Australia

<sup>4</sup>Advanced Photon Source, Argonne National Laboratory, Argonne, IL 60439, USA

<sup>5</sup>Center for Nanoscale Materials, Argonne National Laboratory, Argonne, IL 60439, USA

**Abstract** — The root cause of light- and elevated temperature-induced degradation (LeTID) in multicrystalline silicon *p*-type passivated emitter and rear cell (PERC) devices is still unknown. Some researchers hypothesize that high temperature firing processes dissolve metal-rich precipitates which can then participate in LeTID. To address this hypothesis, synchrotron-based X-ray techniques, including fluorescence and absorption near-edge spectroscopy, are employed. In as-grown industrial material, we observe collocated copper- and nickel-rich precipitates, which persist after firing and are below the detection limit after phosphorous diffusion. We conclude that precipitates decrease in size due to the firing process and that this may result in an increase in bulk interstitial metal concentration. We further employ microphotoluminescence at a grain versus grain boundary to highlight similarities and possible differences in degradation and regeneration behavior.

**Index Terms** — Degradation, light-induced degradation, carrier-induced degradation, copper, nickel, precipitate, synchrotron, photoluminescence, multicrystalline silicon, materials reliability, passivated emitter and rear cell (PERC), silicon, characterization.

## I. *P*-TYPE PERC LETID & METALS

Light- and elevated temperature-induced degradation (LeTID, otherwise known as carrier-induced degradation or CID) can cause about 10% relative efficiency degradation in multicrystalline silicon (mc-Si) passivated emitter and rear cell (PERC) devices during the first months of operation [1]. In the field, this degradation can take many years to recover, representing a significant loss to installed system energy yield over time [2]. While mitigation strategies for LeTID have been suggested with varying success, the root cause of LeTID is still unknown.

The cause of LeTID is thought to be a uniformly distributed bulk defect, and lifetime spectroscopy results point to a metastable deep-level donor/hydrogen complex [3]. However, some spatial inhomogeneity has been noted in the rate and extent of both degradation and regeneration [4]. Recently, Luka *et al.* confirmed the presence of Cu-containing precipitates at grain boundaries and at the rear surface of LeTID-sensitive

solar cells after degradation [5]. The authors hypothesized that Cu originated from the mc-Si wafer, rather than deposited layers or processing equipment. Researchers have further suggested that high-temperature firing processes, after which LeTID is observed, dissolve metal precipitates and introduce interstitial atoms to the bulk which can then participate in the LeTID reaction [6].

In this contribution, we employ PL imaging and synchrotron-based elemental characterization to study precipitate distributions at a grain boundary in the as-grown state and after processing to further investigate both precipitate dissolution during firing and spatial inhomogeneity in LeTID-affected material. We observe Cu- and Ni-rich particles with micro-X-ray fluorescence ( $\mu$ -XRF), and we characterize the collocation of these particles with both micro-X-ray absorption near-edge spectroscopy ( $\mu$ -XANES) and higher resolution nano-XRF. Our results indicate that as-grown metal-rich precipitates may supply interstitial metals to the bulk during high temperature processes, which may then participate in the LeTID reaction. We further hypothesize that metal-rich precipitates inhibit hydrogenation at the studied grain boundary. Using microscale photoluminescence (PL) measured throughout degradation, we demonstrate similarities and possible differences in LeTID between grains and grain boundaries.

## II. METHODS: $\mu$ -XRF, NANO-XRF, PLI, AND *IN SITU* $\mu$ -PL

All samples used in this study are industrial *p*-type mc-Si grown by directional solidification, known to exhibit LeTID. For synchrotron-based experiments, six nearly-adjacent wafers were subjected to various processing steps: (1) as-grown, (2) fired at 620°C (low firing, setpoint), (3) fired at 850°C (high firing, setpoint), (4) phosphorous diffusion gettering (PDG), (5) PDG followed by low firing, and (6) PDG followed by high firing. The sample temperature during firing is approximately 10-20°C below the setpoint temperature. All wafers were saw-damage etched and cleaned prior to processing, and  $\text{AlO}_x/\text{SiN}_y$  (350°C, PECVD) was used to passivate all wafers. Photoluminescence imaging (PLI) was employed to evaluate

electrical performance. Spatially-resolved  $\mu$ -XRF maps were measured at beamline 2-ID-D at the Advanced Photon Source in 220 nm steps with a 200 nm spot size. At select metal-rich particles,  $\mu$ -XANES measurements were conducted to discern chemical structure. High resolution nano-XRF maps of metal-rich particles were measured at beamline 26-ID-C in 10 nm steps with a 30 nm spot size [7].

Micro-photoluminescence ( $\mu$ -PL) was measured using a Horiba LabRAM system, equipped with a confocal microscope and a temperature stage. Several measurements at grains and grain boundaries were conducted *in situ* during accelerated degradation at 140°C with illumination from a 36 mW, 532 nm light source with a spot size of approximately 2.5  $\mu$ m ( $\approx 7 \times 10^6$  suns). The detection area ( $\approx 10 \mu$ m) is governed by carrier diffusion away from the illuminated spot during the measurement. A PERC semiconductor fired at 950°C, previously studied in [3], was chemically stripped of all dielectric layers and passivated with an  $\text{AlO}_x/\text{SiN}_y$  stack. Prior to  $\mu$ -PL measurements, the sample was annealed in the dark for 10 minutes at 200°C to ensure a representative initial state.

### III. SYNCHROTRON-BASED RESULTS

Synchrotron-based  $\mu$ -XRF maps of the  $\text{Cu-K}\alpha$  and  $\text{Ni-K}\alpha$  fluorescence at the same grain boundary in each sample are shown in Fig. 1 (log scale). Pixels with high metal concentration are white, while pixels with low metal concentration are dark red. For the as-grown, low firing, and high firing measurements, Cu- and Ni-rich particles can be identified along the grain boundary. After PDG, only one localized Cu particle can be observed visually, while the remaining particles have dissolved and/or been externally getterred to below the technique detection limit.

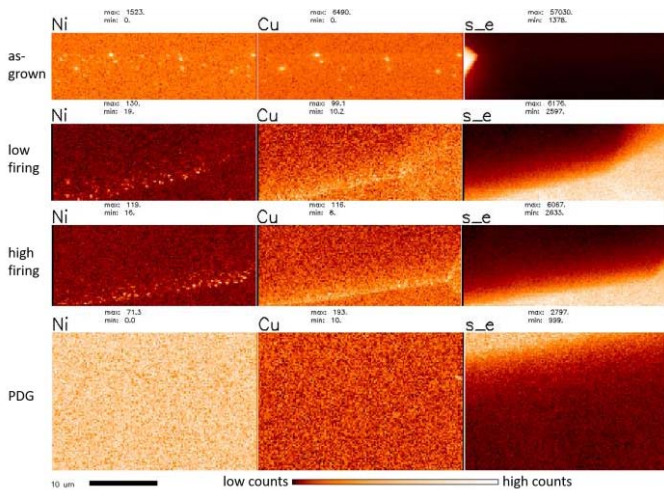


Fig. 1:  $\mu$ -XRF maps of  $\text{Cu-K}\alpha$  fluorescence (left) and  $\text{Ni-K}\alpha$  fluorescence (middle), and elastically-scattered photons (right) for samples after different processing steps. The elastic maps demonstrate the location of the grain boundary during the measurement. Each map is 30  $\mu$ m wide.

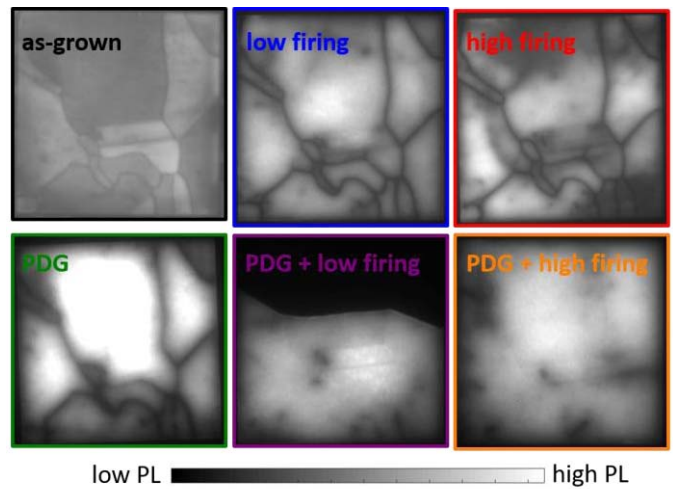


Fig. 2: Photoluminescence images of the samples measured by  $\mu$ -XRF. Images have been scaled for visibility; relative brightness between samples does not indicate a lifetime difference. All samples are 1  $\text{cm}^2$ , except for the PDG + low firing sample, which was broken during the measurement.

In the maps shown in Fig. 1, Cu and Ni are observed in the same pixel for both as-grown and processed samples. However, due to the beam spot size at 2-ID-D, no further information about possible collocation can be discerned. Nano-XRF maps (not shown) of  $\text{Cu-}$  and  $\text{Ni-K}\alpha$  fluorescence of select particles from the same grain boundary indicate that Cu and Ni are present in the same location, but there is a portion of the particle which contains Cu only. Furthermore, the two Cu clusters are oriented nearly perpendicular to each other. To further assess the nature of these particles,  $\mu$ -XANES measurements of a representative particle were collected (not shown). The measured spectra are similar in absorption onset and shape to a  $\text{Cu}_3\text{Si}$  standard, reported in Ref. [8].

Photoluminescence images of the same samples measured with  $\mu$ -XRF (Fig. 2) demonstrate that all processes increase the lifetime at the measured grain boundary, with the highest lifetime achieved by PDG. In all as-grown samples and the sample directly after PDG, the grain boundary can still be observed as recombination-active. However, for the samples subjected to PDG followed by low/high firing, the lifetime is further increased and the grain boundary can no longer be observed in PLI, suggesting that the grain boundary was rendered non-recombination active by the firing process.

### IV. MICROPHOTOLUMINESCENCE RESULTS

Several authors have suggested that, while the defect responsible for LeTID is most likely present throughout the entire wafer, both degradation and regeneration start locally and spread across the wafer. To assess this inhomogeneity, especially in the context of the inhomogeneous metal distributions shown in Fig. 1, one representative set of  $\mu$ -PL measurements, at a grain boundary and inside a grain, is shown in Fig. 3. Both measurements are normalized to the initial value

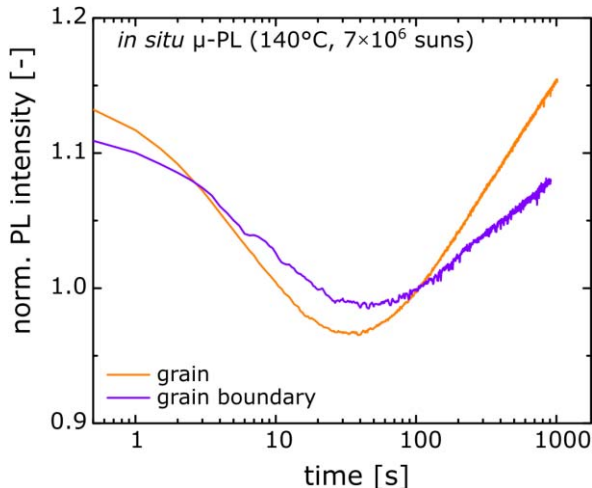


Fig. 3:  $\mu$ -PL measurements of a sample, sensitive to LeTID, under accelerated degradation conditions (140°C,  $\approx 7 \times 10^6$  suns). Measurements were performed separately with the spot centered inside a grain and then centered on a grain boundary.

at  $t = 0$  seconds. Both the rate and extent of degradation are similar for the grain and grain boundary. The similarity in behaviors supports the hypothesis that the LeTID defect is homogeneously distributed across the wafer, and suggests that inhomogeneous distributions of metal-rich precipitates like those observed by  $\mu$ -XRF are unrelated to LeTID. However, there is a notable difference in regeneration behavior: the grain boundary exhibits both a slower initial degradation and regeneration than the grain. These differences may be due to an inhomogeneous LeTID defect distribution or to a lower injection level at and around the grain boundary.

## V. DISCUSSION

The  $\mu$ -XRF measurements confirm the presence of both Cu- and Ni-rich precipitates at a grain boundary in industry-relevant mc-Si material affected by LeTID, suggested by Luka *et al.* [5]. Although Cu-LID as reported in the literature does not describe LeTID [9], certain Cu- and/or Ni-containing complexes which have not yet been studied may be involved in LeTID.

After firing, we observe a reduction in precipitate size, which could correspond to an increase in interstitial atoms available throughout the wafer to participate in LeTID. The presence of metals at an as-grown grain boundary and the reduction in number and size of metal-rich precipitates after PDG has been observed before [10]. However, the persistence of Cu- and Ni-rich particles after firing is unexpected since, in addition to the high diffusivities of these elements at firing temperatures, Buonassisi *et al.* previously observed nearly complete dissolution of Cu- and Ni-rich particles after a rapid thermal anneal at 860°C [11]. The difference in observations can be explained by a difference in sample processing temperature, by a difference in initial precipitate distributions (higher

precipitate density at the grain boundary studied herein), and/or by a difference in XRF detection limit.

Additionally, we observe a difference in hydrogenation behavior for grain boundaries with (as-grown) and without (PDG) metal-rich precipitates above the  $\mu$ -XRF detection limit. Since the precipitate size is likely reduced after firing in the as-grown state, a similar trend is expected for precipitates fired after PDG. The grain boundaries are not recombination-active after PDG followed by firing, implying that the presence of metal-rich precipitates above the  $\mu$ -XRF detection limit impeded passivation by hydrogen in the as-grown samples.

## VI. SUMMARY

We present microscale elemental and electrical characterization of grain boundaries in industrial *p*-type multicrystalline silicon, known to be sensitive to LeTID. We draw two main conclusions from this work: 1) metal-rich precipitates are present in today's industry standard mc-Si material sensitive to LeTID, and 2) sufficiently large precipitates of fast-diffusing metals such as Cu and Ni are not fully-dissolved by high-temperature firing processes. We hypothesize that metal-rich precipitates may inhibit hydrogenation at grain boundaries and interfere with LeTID reactions, causing some spatial inhomogeneity.

## ACKNOWLEDGEMENT

This material is based upon work supported by the National Science Foundation (NSF) and the Department of Energy (DOE) under NSF CA No. EEC-1041895. This work made use of the Center for Nanoscale Systems, Harvard University, supported by National Science Foundation (NSF) Award ECS-0335765. M. A. Jensen and E. E Looney acknowledge support by the National Science Foundation Graduate Research Fellowship under Grant No. 1122374. M. A. Jensen acknowledges support by the National Science Foundation Graduate Research Opportunities Worldwide fellowship for travel to Australia. This research used resources of the Advanced Photon Source, a U.S. Department of Energy (DOE) Office of Science User Facility operated for the DOE Office of Science by Argonne National Laboratory under Contract No. DE-AC02-06CH11357. Use of the Advanced Photon Source and the Center for Nanoscale Materials was supported by the U. S. Department of Energy, Office of Science, Office of Basic Energy Sciences, under contract DE-AC02-06CH11357.

## REFERENCES

- [1] K. Ramspeck *et al.*, "Light induced degradation of rear passivated mc-Si solar cells," in *Proceedings of the 27th European Photovoltaic Solar Energy Conference*, 2012, pp. 861–865.
- [2] F. Kersten *et al.*, "Degradation of multicrystalline silicon solar cells and modules after illumination at elevated temperature," *Sol. Energy Mater. Sol. Cells*, vol. 142, pp. 83–86, 2015.
- [3] K. Nakayashiki *et al.*, "Engineering Solutions and Root-Cause Analysis for Light-Induced Degradation in *p*-Type

- Multicrystalline Silicon PERC Modules,” *IEEE J. Photovoltaics*, vol. 6, no. 4, pp. 860–868, 2016.
- [4] A. Zuschlag, D. Skorka, and G. Hahn, “Degradation and regeneration in mc-Si after different gettering steps,” *Prog. Photovolt Res. Appl.*, 2016.
- [5] T. Luka, M. Turek, S. Großer, and C. Hagendorf, “Microstructural identification of Cu in solar cells sensitive to light-induced degradation,” *Phys. status solidi - Rapid Res. Lett.*, vol. 5, pp. 1–5, 2017.
- [6] R. Eberle, W. Kwapil, F. Schindler, M. C. Schubert, and S. W. Glunz, “Impact of the firing temperature profile on light induced degradation of multicrystalline silicon,” *Phys. status solidi - Rapid Res. Lett.*, vol. 5, pp. 1–5, 2016.
- [7] R. P. Winarski *et al.*, “A hard X-ray nanoprobe beamline for nanoscale microscopy,” *J. Synchrotron Radiat.*, vol. 19, no. 6, pp. 1056–1060, 2012.
- [8] T. Buonassisi *et al.*, “Transition metal co-precipitation mechanisms in silicon,” *Acta Mater.*, vol. 55, no. 18, pp. 6119–6126, 2007.
- [9] A. Inglese, J. Lindroos, H. Vahlman, and H. Savin, “Recombination activity of light-activated copper defects in p-type silicon studied by injection- and temperature-dependent lifetime spectroscopy,” *J. Appl. Phys.*, vol. 120, no. 12, p. 125703, 2016.
- [10] A. E. Morishige *et al.*, “Synchrotron-based investigation of transition-metal getterability in n -type multicrystalline silicon,” *Appl. Phys. Lett.*, vol. 108, no. 20, 2016.
- [11] T. Buonassisi *et al.*, “Impact of metal silicide precipitate dissolution during rapid thermal processing of multicrystalline silicon solar cells,” *Appl. Phys. Lett.*, vol. 87, no. 12, pp. 1–3, 2005.